University *of Ljubljana*
Faculty of *Mathematics and Physics*

Seminar I - 1st year, 2nd cycle degrees

Tip-enhanced Raman Spectroscopy

Author: Nika Šturm
Mentor: prof. dr. Irena Drevenšek

Kranj, may 2019

Abstract

Tip-enhanced Raman spectroscopy (TERS) combines chemical sensitivity of Raman scattering and signal enhancement at nanoroughened metal surfaces with a high spatial resolution of scanning probe microscopies (SPM) and consequently enables chemical imaging of surfaces at the nanometre length-scale.

Contents

1 Introduction

Due to their unusual chemical, electronic and mechanical properties, which are different from their bulk counterparts, materials' surfaces and other atomically thin two dimensional layers have been extensively studied in the past. However, it is still challenging to investigate biological samples with nanoscale spatial resolution, especially in a label-free and non-destructive way [1].

Well-established nanoscale characterization techniques, such as electron and various scanning probe microscopies (SPM), provide information on surface topography and some electro-magnetic properties, but they offer almost no chemical sensitivity [2]. That might not be entirely true for methods such as energy dispersive X-ray spectroscopy (EDX), but EDX requires that all samples are analysed under relatively high vacuum and this has serious implications for the sample preparation [3]. On the other hand, Raman effect provides rich information on the sample chemical structure and can be done in ambient conditions. Due to its very low scatterig cross-section, a minimal amount of material that can be analyzed is quite limited. Additional drawback of Raman spectroscopy is its spatial resolution, which is defined by the diffraction limit of light [4].

There are several methods to enhance the signal, such as resonant and interference-enhanced Raman scattering [5], but major progress came with the invention of surface-enhanced Raman scattering (SERS) [6] and use of nanoplasmonics [7], which can enhance the Raman signal up to 10^{14} times. Combining signal enhancement with high spatial resolution of SPM, leads to a relatively new technique for surface imaging at the nanometre scale; tip-enhanced Raman spectroscopy (TERS). Each pixel in the scanned image contains full vibrational spectroscopic information on the sample region imaged into that pixel. A specific vibrational mode can be selected to construct an image that shows spatial distribution of a particular molecule. By overlaying several images

corresponding to various vibrational modes, a full mapping of chemical composition over large sample area can be obtained. The size of imaged area depends on SPM technique [8].

In this seminar I will explain basics of Raman scattering, then briefly describe enhancement mechanisms of SERS and after this I will discuss some of the technical aspects of TERS.

2 Raman Scattering

Scattering can be broadly described as redirection of electromagnetic radiation from the original path of propagation, due to localized non-uniformities in the medium through which it passes, such as molecules, particles, droplets, density fluctuations and defects in crystals. When material is illuminated by an incident electromagnetic wave, its atoms or molecules can be excited into a virtual energy state by absorption of a photon. This state then relaxes and creates another photon through a scattering process, which can either be elastic (Rayleigh and Mie scattering), or inelastic (Brillouin, inelastic X-ray, Compton and Raman scattering) [9].

The Raman effect, which was experimentally discovered in 1928 by C.V. Raman, creates a photon with either lower energy $\hbar(\omega_0 - \omega_v)$ than the incident photon, and this is called Stokes scattering, or with higher energy $\hbar(\omega_0 + \omega_v)$, so-called anti-Stokes scattering (Figure 1, top). Incident photon energy is denoted as $\hbar\omega_0$, and $\hbar\omega_v$ is the vibrational or rotational energy of a molecule (or a phonon state in a crystal). Scattered light can also have a different polarization from the incident light. If the intermediate virtual energy level coincides with one of the real molecular electronic states, the process is called the resonance Raman effect. The energy difference between the incident and the scattered light can be analysed in order to obtain a vibrational spectrum of a sample [5].

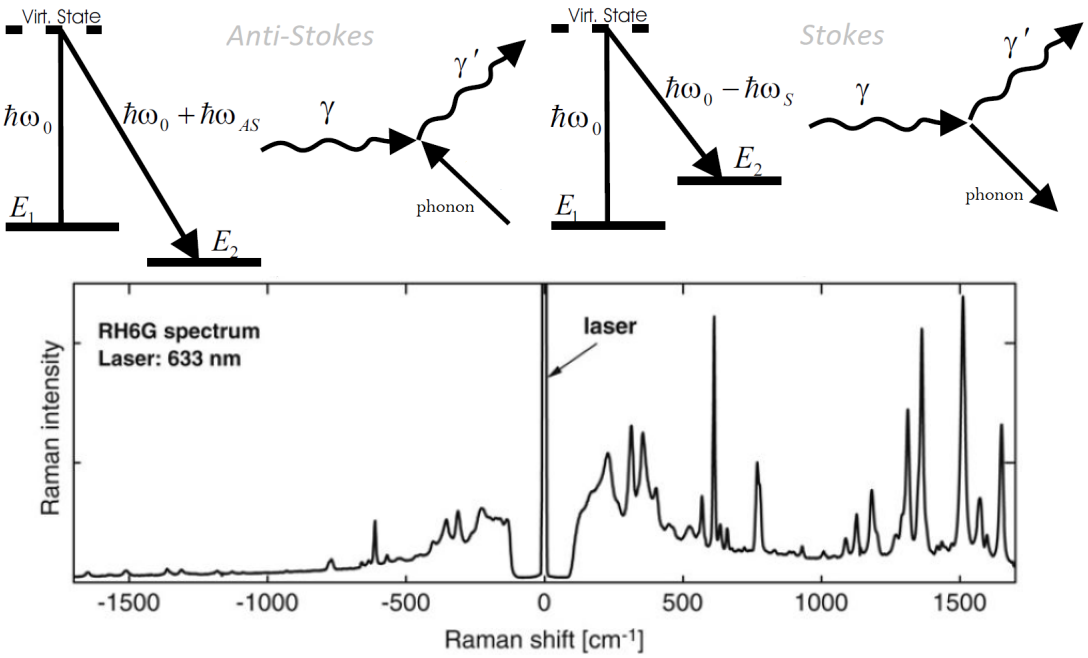

Figure 1: Top: Shematic diagrams of anti-Stokes and Stokes processes with assigned Feynman diagrams. Adapted from [10]. Bottom: Raman spectrum for rhodamine 6G. Anti-Stokes emission lines are in the negative part of the Raman shifts scale. Adapted from [11].

2.1 Classical theory of Raman effect

The origin of the scattered radiation are induced electric dipoles in the material. A classical description of the vibrational Raman effect starts from the relation:

$$\mathbf{p} = \boldsymbol{\mu} + \underline{\alpha}\mathbf{E}, \tag{1}$$

where $\boldsymbol{E} = \boldsymbol{E_0}\cos(\omega t)$ is electric field of the incident wave, $\mathbf{p}$ is the dipole moment of a molecule, $\boldsymbol{\mu}$ represents a permanent dipole moment and $\underline{\alpha}\mathbf{E}$ is the induced dipole moment [(i)]. Dipole moment and polarizability are functions of nuclear coordinates. If the frequency of incident radiation is far off resonance with electronic transitions, the nuclear displacements are small and so they can be expanded into Taylor series in the normal coordinates q_n of the nuclear displacements:

$$\boldsymbol{\mu} = \boldsymbol{\mu}(0) + \sum_{n=1}^{Q}\Big(\frac{\partial\boldsymbol{\mu}}{\partial q_n}\Big)_0 q_n + ..., \qquad \alpha_{ij}(q) = \alpha_{ij}(0) + \sum_{n=1}^{Q}\Big(\frac{\partial\alpha_{ij}}{\partial q_n}\Big)_0 q_n + ... \tag{2}$$

where $Q = 3N - 6$ is the number of normal vibrational modes for a molecule with N nuclei, and $\boldsymbol{\mu}(0) = \boldsymbol{\mu}_0$ and $\alpha_{ij}(0)$ are values at the equilibrium configuration $q_n = 0$. For small vibrational amplitudes the normal coordinates $q_n(t)$ of the vibrating molecule can be approximated by:

$$q_n(t) = q_{n0}\cos(\omega_n t), \tag{3}$$

where q_{n0} is the amplitude and ω_n the vibrational frequency of the n-th normal vibrational mode.

If we only consider the first two terms of Taylor expansion, we get the total dipole moment:

$$\begin{aligned}\mathbf{p} &= \boldsymbol{\mu}_0 + \sum_{n=1}^{Q}\Big(\frac{\partial\boldsymbol{\mu}}{\partial q_n}\Big)_0 q_{n0}\cos(\omega_n t) + \alpha_{ij}(0)E_0\cos(\omega t)\\ &+\frac{1}{2}\boldsymbol{E}_0\sum_{n=1}^{Q}\Big(\frac{\partial\alpha_{ij}}{\partial q_n}\Big)_0 q_{n0}\big[\cos((\omega+\omega_n)t) + \cos((\omega-\omega_n)t)\big].\end{aligned} \tag{4}$$

The second term describes the infrared absorption spectrum [(ii)], the third term is the Rayleigh scattering, and the last term represents the Raman scattering. A specific vibrational mode is Raman active, if $(\partial\alpha_{ij}/\partial q_n)_0$ has a non-zero value.

Although the classical theory correctly describes the frequencies $\omega \pm \omega_n$ of the Raman lines, it fails to give their correct intensities and the use of quantum mechanics is required. The intensity of a selected Raman line is determined by the population density $N_i(E_i)$ of molecules in the initial energy level E_i, by the intensity I_L of incident optical beam and by the Raman scattering cross section σ_R as:

$$I_s = N_i(E_i)\sigma_R(i \to f)I_L. \tag{5}$$

[(i)] The polarizability tensor $\underline{\alpha}$ is real and symmetrical tensor of second rang [10]. It depends on the molecular symmetry; the matrix elements $\langle\alpha_{ij}\rangle$ depend on the symmetry characteristics of the molecular states. While the theoretical evaluation of the magnitude of $\langle\alpha_{ij}\rangle$ demands a knowledge of the corresponding wave functions, the question whether $\langle\alpha_{ij}\rangle$ is zero or not depends on the symmetry properties of the molecular wave functions for the states $|i\rangle$ and $|f\rangle$ and can therefore be answered by group theory without explicitly calculating the matrix elements [5]. A more detailed explanation can be found in [12].

[(ii)] In a molecule with a center of symmetry it is seen that vibrations that are Raman active are IR inactive and vice-versa, this is called the Principle of mutual exclusion. In molecules with different elements of symmetry, certain bands may be active in IR, Raman, both or neither. For a complex molecule that has no symmetry except identity element, all of the normal modes are active in both IR and Raman. In general the strong bands in the IR spectrum of a compound corresponds to weak bands in the Raman and vice versa [13].

At thermal equilibrium, the population density $N_i(E_i)$ follows the Boltzmann distribution. Consequently anti-Stokes Raman process is generally far less intense than Stokes Raman process (by factor $e^{-\hbar\omega_v/k_BT}$), and this can be seen on Figure 1 (bottom).

When the intensity of incident optical beam becomes sufficiently large, the induced oscillation of the electron cloud surpasses the assumed linear approximation and non-linear regime needs to be considered, in which $\boldsymbol{p(E)}$ is expanded into a power series of $\boldsymbol{E}$ [5].

2.2 Raman spectroscopy

Raman spectroscopy is a non-destructive analytical technique, which often requires no specific sample preparation. It can be applied in challenging environments such as deep ocean waters and space exploration and is useful in medicine, forensic sciences, art, food quality control, analytical chemistry, nanomaterials, geological investigations, crystal analysis, etc. [2].

It has two main disadvantages: the achievable spatial resolution is restricted by the diffraction limit and the Raman effect is an exceedingly weak phenomenon, as the predominant scattering process is Rayleigh scattering. Typical Raman cross sections are 10^{-30} to 10^{-25} cm^2, with the larger values occurring during resonant Raman conditions. For comparison, fluorescence spectroscopy has effective cross sections between 10^{-17} and 10^{-16} cm^2 [6].

3 Surface enhanced Raman scattering

The intensity of Raman scattered light can be enhanced by several orders of magnitude if the molecules are adsorbed on a nano-roughened metallic surface. The enhancement effects depend on the orientation of the molecules relative to the surface normal, on the size and shape of underlying metallic particles and on the frequency, power and polarisation of incident light. Several mechanisms contribute to this enhancement [6].

3.1 Electromagnetic enhancement

The primary mechanism is EM enhancement, which can produce enhancement factor of $10^8 - 10^{11}$ [8]. It is based on the same phenomena as beautiful colours of stained-glass windows in old cathedrals: on the resonant excitation of surface plasmons in metallic nanostructures [7].

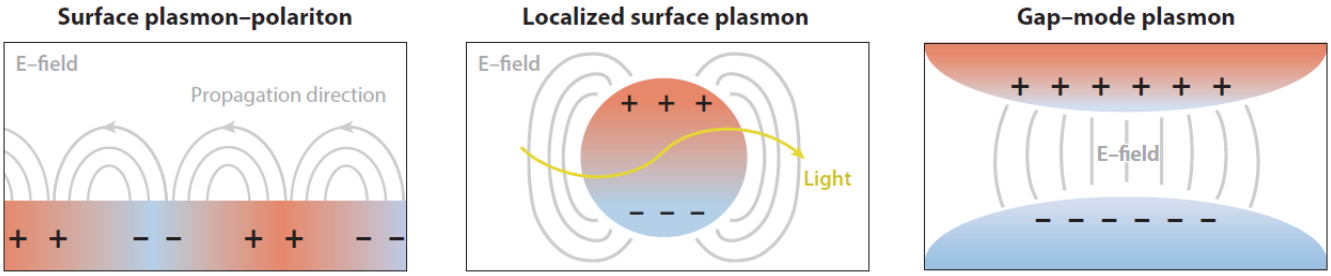

Figure 2: Charge and field distributions of basic plasmon resonance modes. Rep. from [14].

The simplest model of a molecule positioned near a metal sphere, with dimensions smaller than the wavelength of incident light, describes most of the properties of EM SERS effect. Time varying electrical field of light penetrates the sphere and causes displacement of electrons with respect

to the lattice, which results in opposite charges appearing on the opposite sides of the sphere. Attraction of those charges causes collective oscillations of free electrons in a material, called plasmons. Plasmons are quasiparticles, the quantum form of non-propagating or evanescent optical fields, analogous to photons (quantum form of propagating light) or phonons (latice exitations) [7]. They are confined to a metal-dielectric interface, e.g., on flat surfaces or nanostructures or within a nanoscale dielectric gap, as shown in Figure 2.

The magnitude of surface plasmon field E_{SP} at the position of the molecule depends on the sphere's radius a, its distance from the molecule r, the metal's complex dielectric constant ε_{in}, dielectric constant of surrounding medium ε_{out} and on the amplitude of incident optical field E_0. It can be approximated by:

$$E_{out}(x,y,z) = E_0\hat{\boldsymbol{z}} + \Big[\frac{\varepsilon_{in}-\varepsilon_{out}}{\varepsilon_{in}+2\varepsilon_{out}}\Big]a^3E_0\Big[\frac{3z}{r^5}(x\hat{\boldsymbol{x}}+y\hat{\boldsymbol{y}}+z\hat{\boldsymbol{z}}) - \frac{\hat{\boldsymbol{z}}}{r^3}\Big]. \tag{6}$$

Step by step deduction of this equation can be found in supplemental appendix of [15].

The molecule feels the enhanced local field, which is the sum of incident and plasmon fields. This enhancement is particularly strong when a real part of ε_{in} is equal to $-2\varepsilon_{out}$[(iii)], which is the condition for resonant excitation, and when the imaginary part of ε_{in} is small. If the plasmon resonance is broad enough to cover both, the incident and Raman scattered wavelengths, then both can be simultaneously enhanced, resulting in much larger enhancement than if only one of them is enhanced [6, 16]. Spatial distribution of highly localized electrical fields is inhomogeneous. Intensity spikes, that arise from multiplication of enhancement factors due to various SP resonances, constructive interference of fields from diferent SPs and specific geometries such as sharp tips or narrow gaps are called hot spots. The most exploited hot spot is the one due to the lightning rod effect - a sharp tip at which a high local field is produced when the polarization of the exciting light is parallel to the tip's axis. For spheres with sizes comparable to or larger than the wavelength of the incident light, the field over the nanoparticle volume is not homogeneous and higher order multipoles are induced. A precise solution for such situations is referred to as Mie theory [2].

3.2 Chemical enhancement

The electronic interaction between the selected molecule and the underlying metal can modify the scattering process itself and produce an effectively larger Raman scattering cross-section than would occur by the scattering from the molecule alone - this is known as chemical or electronic enhancement and it contributes to the enhancement by a factor of about $10^2 - 10^3$ [8]. The true origin of the chemical enhancement is still not completely understood, but is usually interpreted by the charge-transfer (CT) mechanism. The molecule is covalently bound to the metal surface, which modifies the existing electronic structure and changes the intrinsic polarizability of the molecule. It is also possible that a new electronic state is created close to the resonance with the incident light frequency creating a resonant Raman scattering. Such modifications of the Raman polarizability tensor can lead to either enhancement or damping of the signal and are also likely to cause the changes in the Raman spectra (change in relative Raman bands intensities and positions) due to perturbations of the material structure. [2]

[(iii)] At high frequencies metals act like a plasma. Noble metals (gold, silver) show negative permittivity at optical frequencies.

4 TERS - tip enhanced Raman spectroscopy

While SERS immensely enhances the Raman signal, it does not improve its spatial resolution. Even though SERS is a near-field phenomenon, the enhanced field is confined only in the direction perpendicular to the roughened metallic surface. Metallic surfaces used in SERS are typically very large, so the lateral confinement of the light is defined by the spot size of incident focused laser beam. [1]

The concept of TERS was first proposed by J. Wessel in 1985 [17] and was experimentally realised by different groups in 2000 [18–20]. It combines the chemical selectivity of Raman, the high sensitivity of SERS and the lateral resolution of scanning probe microscopy. The scanning tip also provides complementary topographic information of the sample [4].

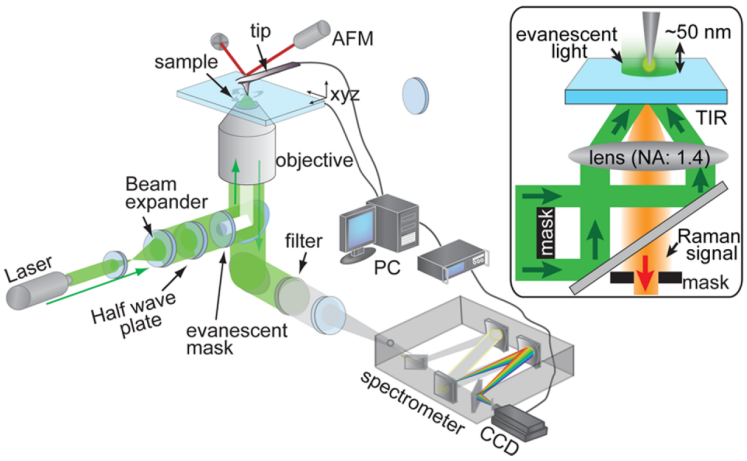

Figure 3: Illustration of a typical AFM-based TERS measurement system. Inset shows the details of the sample illumination process. Reproduced from [8].

4.1 TERS enhancement

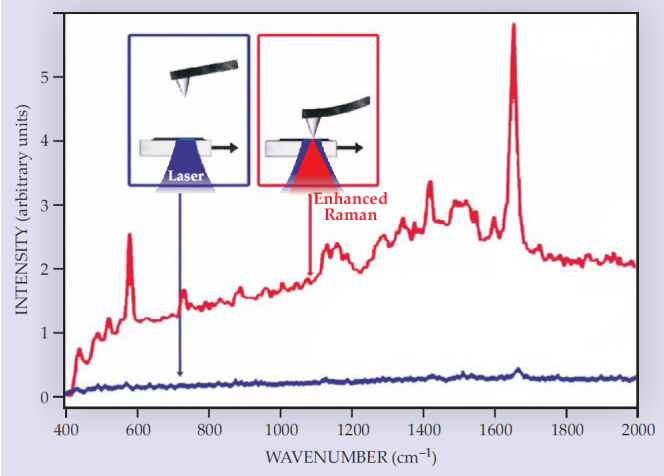

Figure 4: Two Raman spectra of brilliant cresyl blue dye molecules dispersed on glass; blue - far-field, red - near-field. Rep. from [6].

In TERS, metallic nano-roughened surface from SERS is replaced by the single metal tip. The enhancement mechanisms are largely the same as those in SERS, but the total enhancement is smaller as there is no constructive interference due to neighbouring nanoparticles. Since the sample molecules are not adsorbed on the metallic surface, the chemical enhancement is also smaller. However, the tip behaves like a single antenna or a point enhancer, so lightning rod effect is present, when the probe antenna has high local curvature over distances much smaller than the wavelength of light (e.g., corners, sharp edges, small gaps). The sharp boundaries of the probe restrict the motion of electrons, causing charge concentration along the probe surface [1].

An enhanced Raman signal is generated from a tiny volume of the sample right below the tip and is excited by the nanolight-source created at the tip apex, which gives the so-called near-field signal. At the same time, Raman signal is also generated from the entire illuminated focal spot, which gives the far-field signal. Collected signal is a combination of both, so measurements

are done in two steps. First, Raman signal is collected when the tip is close to the surface and then again when the tip is vertically retracted from the sample, usually by several hundreds of nanometres, as shown in figure 4. By subtracting far-field signal from the near-field one, a pure near-field Raman scattering signal is obtained [8].

The associated enhancement factor (EF) is difficult to estimate and measure, as it depends on several parameters. Further details of tip-enhancement can be found in the book by S. Kawata and V. M. Shalaev [21]. Most commonly EF is calculated as:

$$EF = (\frac{I_{tip-in}}{I_{tip-out}} - 1)\frac{A_{FF}}{A_{NF}} \tag{7}$$

where I_{Tip-in} and $I_{Tip-out}$ are scattering intensities measured with the tip approached and retracted from the sample, respectively. A_{FF} is the area of a far-field laser probe and A_{NF} is the effective area of a TERS probe, which is usually estimated from the geometric diameter of the tip-apex [4].

4.2 Spatial Resolution

In optical microscopy, the spatial resolution Δx is a minimal distance between two objects, such that they can still be distinguished in the image. Abbe or Rayleigh criterion estimates the spatial resolution as $\Delta x = 0.61\lambda/NA$, where λ is the wavelength of light and NA is the numerical aperture of the objective. The value of Δx is often approximated as half the irradiation wavelength, which gives resolution of $200 - 300$ nm when using visible light [1].

In TERS, the diffraction limit does not play a role as its spatial resolution depends on the field confinement, which is determined by the size of tip apex. Generally, resolution of 10–80 nm has been reported, which is in accordance with the diameter of a typical SPM tip apex. In such a context, the spatial resolution of TERS should simply be limited by the geometry of the tip apex, but recently several experiments have shown unprecedented TERS spatial resolution down to the sub-nanometer regime, examples can be found in [22–25]. This surprisingly good spatial resolution cannot be explained by the size, shape and material of the nanotip at the apex, therefore mechanisms underlying the subnanometer spatial resolution of TERS are at present not yet understood [1].

4.3 Technical aspects

4.3.1 Optical set-up for TERS

As a typical Raman spectroscopy setup, the TERS set-up consists of an excitation laser, a microscope objective (usually equipped with a high-NA lens for tight focusing), a sample stage, a spectrometer and a CCD detector, as shown in Figure 3. In addition, the sample stage is equipped with a SPM controller to position a metallic nanotip on the sample surface within the laser focus. Since intensity distribution within the focal spot is not uniform, it is very important to lock the relative position of the focus and the tip [8].

There exist various configurations to illuminate the sample and collect Raman signal that are shown in Figure 5. In the sample illumination process a special mask is used, so that the low-NA component at the center of the beam is blocked and only a high-NA component goes through the objective to create a total internal reflection at the substrate surface. This ensures that the incident light does not transmit through the substrate, which reduces the unwanted background signal from the propagating light. Since the evanescent light decays within a few tens of nanometres

from the surface, it also ensures that only the tip apex is illuminated, which creates a nanolight-source. The Raman scattered signal is collected by the same objective and any possible reflected light is rejected by another apertured mask that allows only the low-NA component to enter the spectrometer [8].

The quality of a TERS set-up depends on two characteristics of the probe tip; on its abilities to enhance and to confine the light field at the tip apex.

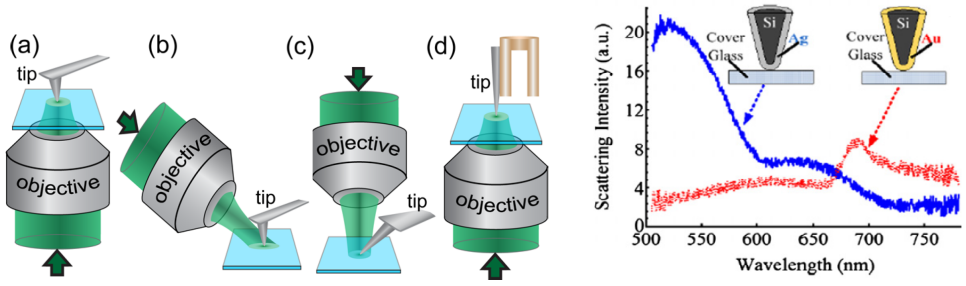

Figure 5: Left: (a)Back illumination transmission mode with backscattering geometry, (b) side illumination, (c) top illumination, (d) transmission mode. Rep. from [8]. Right: Scattering of light from silver- and gold-coated AFM tips. Reproduced from [4].

4.3.2 Tip choice

Plasmon resonance wavelength and enhancement factor are determined by the choice of a tip metal. Both are also dependent on the radius of the tip-apex and on the morphology of evaporated metal on the tip surface. Gold shows strong enhancement in the red, silver has better results in the blue-green (figure 5) and aluminium has promising results in the UV spectral region. Gold is very stable under the ambient condition and gold-coated tips can survive for a long time, while silver can easily get oxidized and the tip lasts only a few hours [8].

If the achievable resolution is defined by the tip apex radius, then the tip size needs to be minimized. On the other hand there is also an opinion, that the tip radii below 10 nm lead to damping of enhancement due to too small amount of available electrons. There are several tip fabrication techniques, the two most commonly applied are electrochemical etching and metal coating [4].

4.3.3 Scaning Probe Microscopies

There are three major SPM systems used for TERS, which are based on scanning tunneling microscopy (STM), atomic force microscopy (AFM), or shear force microscopy. Each of them has certain advantages over the others. STM-based TERS has the advantage of a high spatial resolution associated with the STM technique and allows high-vacuum and low-temperature measurements. Its disadvantage is that the sample is placed on a thick metallic substrate, therefore it is not possible to use the transmission mode with backscattering configuration. AFM system is more versatile in terms of usage for both, non-conductive and conductive samples and can also be used in transmission mode. It can operate in ambient conditions, and also in liquid environment. This is particularly interesting for biological samples, because it allows nano-imaging under physiologically relevant conditions. [4, 8]

4.4 Applications: TERS imaging of 2D materials

TERS imaging is becoming a viable technique to obtain molecular distribution and local concentration over the large area of the sample with a nanoscale resolution. Imaging is performed by raster scanning the sample stage by means of piezoelectric controllers with SPM feedback loop, while obtaining topography and Raman spectrum at each pixel.

TERS imaging is affected by spectral and spatial resolution artefacts that occur due to thermal drift, thermal diffusion and tip degradation. Thermal drift is unavoidable under ambient conditions; a compromise between the acquisition time of each pixel and the step size has to be found, but that may lower the spatial resolution. Laser and near-field heating of the substrate can lead to fluctuations of molecular orientation, desorption, movements of the sample and even sample decomposition. Consequently some additional signals can occur and peak ratio usually fluctuates in the spectra. Tip degradation can change the morphology and plasmonic properties of the tip, which affects enhancement factor and spatial resolution. Generally, the maximum enhancement of the tip and the highest intensity of the signal is obtained at the beginning of imaging [1].

Over the last two decades, TERS imaging has been used to visualize a distribution of organic molecules in peptide nanochains, to map the structural inhomogeneities of inorganic crystals and track the strain-induced carbon nanotubes (CNTs). An example of TERS image is shown in Figure 6. The technique has also been used to study photovoltaics, catalysis, semiconductors and graphene and recently chemical mapping of single molecules with sub-nanometer spatial resolution was reported [4, 8].

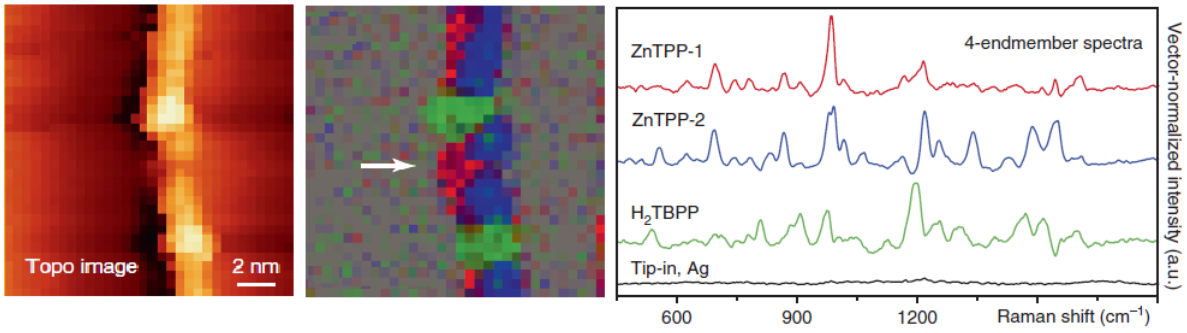

Figure 6: TERS imaging of a mixed molecular chain (porphyrin molecules: ZnTPP-1,2 and H2TBPP) adsorbed at step edges of a silver surface. Left: topography image of the area (simultaneously acquired during TERS imaging, 16×16 nm^2, 32×32 pixels, 0.5 nm per pixel). Middle: TERS image. Right: corresponding Raman spectra for each molecule. Adapted from [22].

5 Conclusion

Although TERS offers numerous advantages for nanoscale chemical characterization, it does have certain limitations. It provides information only about Raman-active molecules and because it is an SPM-based technique, only relatively flat samples can be successfully investigated. The penetration depth of TERS signals is typically less than 10 nm, so only the very top surface of the sample can be analyzed [8]. One of the biggest shortcomings of TERS is the low controllability of the surface morphology and the reproducibility of the tips, due to this quantitative chemical imaging has not yet been achieved.

But despite all that, TERS became a versatile and powerful analytical technique for nanoscale

surface characterization, and recently published Nature Protocol article [26] just goes to show how developed this technique already is. Unlike electron spectroscopy and microscopy techniques (SEM, TEM and XPS) that require vacuum or cryogenic temperatures for their operation, TERS can be used in ambient environment and is label free, which gives it an advantage over the fluorescence microscopy techniques (such as STED), where the fluorescent labels prevent observation of samples in their native state. TERS is rapidly improving its capabilities as a label-free, nondestructive nano-tool,and is belived to become a useful future method for characterization of electronic and optoelectronic devices, as these devices are nowdays shrinking to nanometer size [4].

References

[1] Shao, F. and Zenobi, R. (2018). *Tip-enhanced Raman spectroscopy: principles, practice, and applications to nanospectroscopic imaging of 2D materials.* Analytical and Bioanalytical Chemistry, 411(1), pp.37-61.

[2] Sheremet, E. (2015). *Micro- and Nano-Raman Characterization of Organic and Inorganic Materials.* Doctoral dissertation, Technical University Chemnitz.

[3] Scimeca, M., Bischetti, S. and Lamsira, H. (2018). *Energy Dispersive X-ray (EDX) microanalysis: A powerful tool in biomedical research and diagnosis.* European Journal of Histochemistry, 62(1).

[4] Kumar, N., Mignuzzi, S. and Su, W. (2015). *Tip-enhanced Raman spectroscopy: principles and applications.* EPJ Techniques and Instrumentation, 2(1).

[5] Demtröder, W. (2008) - *Laser Spectroscopy Vol. 2 Experimental Techniques* Springer Berlin Heidelberg, pp. 159-191.

[6] Kneipp, K. (2007). *Surface-enhanced Raman scattering.* Physics Today, 60(11), pp.40-46.

[7] Marin, A. (2012). *Nanoplasmonics - The physics behind the applications* Available at: http://mafija.fmf.uni-lj.si/seminar/files/2011_2012/Nanoplasmonics-The_physics_behind_the_application.pdf [Accessed 24 Apr. 2019].

[8] Verma, P. (2017). *Tip-Enhanced Raman Spectroscopy: Technique and Recent Advances.* Chemical Reviews, 117(9), pp.6447-6466.

[9] Hoch, D. (2015). *Tip-Enhanced Raman Spectroscopy.* Master's thesis, Technische Universität München.

[10] Kunstelj, K. (2004). *Raziskave staranja človeških očesnih leč z Ramansko spektroskopijo* Available at: http://mafija.fmf.uni-lj.si/seminar/files/2003_2004/seminar.pdf [Accessed 14 Apr. 2019].

[11] Le Ru, E. and Etchegoin, P. (2011). *Principles of surface-enhanced raman spectroscopy.* Amsterdam: Elsevier.

[12] Alves, A., Brown, J. and Hollas, J. (1988). *Frontiers of laser spectroscopy of gases.* Dordrecht: Kluwer Academic Publishers, pp.248-258.

[13] Hildebrandt, P. (n.d.). *IR and Raman spectroscopy.* Available at: http://www.fhi-berlin.mpg.de/acnew/department/pages/teaching/pages/teaching__wintersemester__2012_2013/peter_hildebrandt_vibrational_spectroscopy__121123.pdf [Accessed 5 Jun. 2019].

[14] Hermann, R., Gordon, M. (2018). *Nanoscale Optical Microscopy and Spectroscopy Using Near-Field Probes.* Annual Review of Chemical and Biomolecular Engineering, 9(1), pp.365-387.

[15] Willets, K. and Van Duyne, R. (2007). *Localized Surface Plasmon Resonance Spectroscopy and Sensing.* Annual Review of Physical Chemistry, 58(1), pp.267-297.

[16] Zhang, J., Zhang, L. and Xu, W. (2012). *Surface plasmon polaritons: physics and applications.* Journal of Physics D: Applied Physics, 45(11), p.113001.

[17] Wessel, J. (1985). *Surface-enhanced optical microscopy.* Journal of the Optical Society of America B, 2(9), p.1538.

[18] Stöckle, R., Suh, Y. and Deckert, V. (2000). *Nanoscale chemical analysis by tip-enhanced Raman spectroscopy.* Chemical Physics Letters, 318(1-3), pp.131-136.

[19] Anderson, M. (2000). *Locally enhanced Raman spectroscopy with an atomic force microscope.* Applied Physics Letters, 76(21), pp.3130-3132.

[20] Hayazawa, N., Inouye, Y. and Sekkat, Z. (2000). *Metallized tip amplification of near-field Raman scattering.* Optics Communications, 183(1-4), pp.333-336.

[21] Kawata, S. and Shalaev, V. (2011). *Tip Enhancement.* Elsevier Science.

[22] Jiang, S., Zhang, X., Zhang, Y. (2017). *Subnanometer-resolved chemical imaging via multivariate analysis of tip-enhanced Raman maps.* Light: Science and Applications, 6(11), p.e17098.

[23] Zhang, R., Zhang, Y., Dong, Z. and Jiang, S. (2013). *Chemical mapping of a single molecule by plasmon-enhanced Raman scattering.* Nature, 498(7452), pp.82-86.

[24] Lee, J., Crampton, K. and Tallarida, N. (2019). *Visualizing vibrational normal modes of a single molecule with atomically confined light.* Nature, 568(7750), pp.78-82.

[25] Lee, J., Crampton, K., Tallarida, N. and Apkarian, V. (2019). *Visualizing vibrational normal modes of a single molecule with atomically confined light.* Nature, 568(7750), pp.78-82.

[26] Kumar, N. and Weckhuysen, B. (2019). Nanoscale chemical imaging using tip-enhanced Raman spectroscopy. Nature Protocols, 14(4), pp.1169-1193.